Resistance fluctuations in quantum Hall transitions: Network of compressible-incompressible regions

Tomoki Machida
CREST, Japan Science and Technology Corporation, Building 16-622, Komaba 3-8-1, Meguro-ku, Tokyo 153-8902, Japan

Susumu Ishizuka and Susumu Komiyama
Department of Basic Sciences, University of Tokyo, Komaba 3-8-1, Meguro-ku, Tokyo 153-8902, Japan

Koji Muraki and Yoshiro Hirayama
NTT Basic Research Laboratories, 3-1 Morinosato-Wakamiya, Atsugi, Kanagawa 243-0198, Japan
(Received 7 August 2000; published 9 January 2001)

Resistance fluctuations in integer and fractional quantum Hall transitions are studied in modulation-doped $Al_{0.3}Ga_{0.7}As/GaAs$ heterostructures. We examine the role of coherence in the fluctuations by investigating the conductance through two scattering regions that are spatially separated but interact quantum-mechanically with each other. Though the conductor is in a coherent regime, the phase coherence is found to play an insignificant role in determining the observed pattern of fluctuations. In transition regions where the average filling factor of Landau levels takes a noninteger value, $n-1<\nu<n$, the electron system splits into incompressible subregions of $\nu=n$ and those of $\nu=n-1$, which are separated by percolating compressible strips. Irregular evolution of the network of compressible strips is suggested to be the origin of the resistance fluctuations in integer quantum Hall transitions. A similar mechanism is also suggested for fractional quantum-Hall transitions.

DOI: 10.1103/PhysRevB.63.045318 PACS number(s): 73.43.−f, 72.10.−d

I. INTRODUCTION

Conductance fluctuations are one of the key issues in the study of mesoscopic physics.[1] There is a general understanding that the sample-specific conductance fluctuations in weak magnetic fields, the so-called universal conductance fluctuations (UCF), originate from the interference effect between electron waves.[2] Recently, the interest has been extended to the fluctuations in high magnetic field regimes, especially in quantum Hall (QH) transitions.[3–15] Theoretically, the correlation energy and the conductance distribution function of electron systems in QH transitions have been studied.[3–9] Experimentally, resistance fluctuations (RF's) in integer quantum Hall (IQH) transitions are studied,[10–12] where the effects are interpreted as the interference effect among different electron trajectories[10] or as a consequence of resonant tunneling to a small number of localized states.[11–14] In those theoretical and experimental works,[3–14] it is the common prerequisite that the phase coherence of electron systems is the origin of the fluctuations. From the experimental point of view, however, it remains unclear whether the fluctuations in QH transitions are indeed a consequence of coherent processes.

Cobden, Barnes, and Ford[15] studied conductance fluctuations in IQH transitions of silicon metal-oxide-semiconductor field-effect transistors (Si-MOSFET's) and suggested importance of the charging effect, analogous to the Coulomb blockade oscillations in a random network of quantum dots. However, the interpretation is not fully straightforward and questions remain in the physical picture of fluctuations in QH transitions.

In order to shed some more light on the fluctuations in QH transitions, we study here two scattering regions connected in a coherent manner. If the phase coherence determines particular fluctuation patterns in one given region, the patterns should change if the region in study is connected to another scattering region. Surprisingly, we find that the RF pattern of the total (connected) system closely resembles that of the numerical sum of the individual RF patterns, which are separately studied in the respective regions. This is not because of the absence of coherence, but the coherence does not play a substantial role in determining the RF pattern, although it modifies the amplitude of RF's in a characteristic manner. We suggest that the electrostatic-potential profile evolves irregularly with varying physical parameters (such as the gate voltage and magnetic field) and it gives rise to the RF's in QH transitions. This work also provides strong evidence that the two-dimensional electron gas (2DEG) systems at high magnetic fields form a network of subregions in which integer numbers of Landau levels are completely filled even in a regime of IQH transition, where the global longitudinal resistance is finite. Additionally, we show preliminary results of RF's in fractional quantum Hall (FQH) transitions, suggesting a similar mechanism of fluctuations.

II. EXPERIMENTAL METHODS

Samples are Hall bars with two Schottky cross-gates placed in series, as schematically shown in the inset of Fig. 1. They are fabricated on three different wafers of $Al_{0.3}Ga_{0.7}As/GaAs$ heterostructures (I, II, and III) with the electron mobility μ_H and the sheet electron density n_s at 4.2 K of (μ_H [$m^2/V\,s$], n_s [$10^{15}\ m^{-2}$]) = (60, 2.4), (70, 3.5), and (70, 2.9), respectively. Different-size samples are fabricated on one wafer, where the gate length and the channel width are, respectively, (L, W) = (0.4, 4), (0.6, 4), (1, 4), (2, 4), and (3, 3) in units of μm. The distance between the two gates is $L_{edge}=10\ \mu$m for all the samples. Four-terminal measurements are carried out in a ^3He-^4He dilution refrigerator system at temperatures down to 20 mK. Low-pass filters are used inside the mixing chamber as well as outside the cryostat to eliminate the noise heating. The resistance

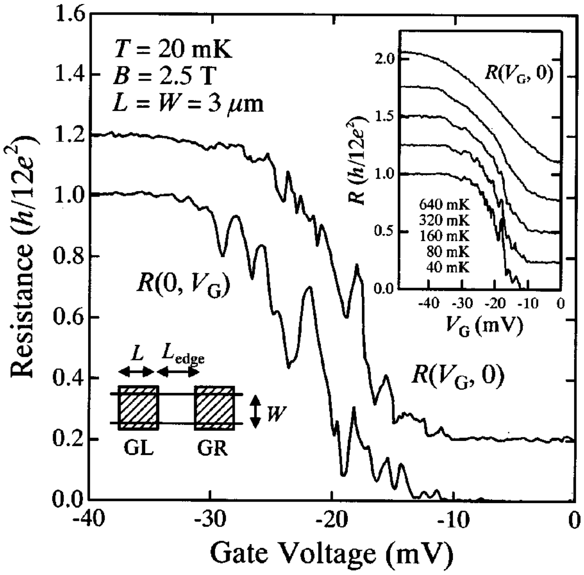

FIG. 1. IQH transition in the resistance $R(V_{\mathrm{GL}},V_{\mathrm{GR}})$ spectrum. Either one of the gates GL (upper) or GR (lower) are biased. The line for GL is offset for clarity. Schematic representation of sample (inset). IQH transition for GL at different temperatures (inset).

values are studied by a standard lock-in technique with an ac current of 1 nA. The differential resistance, $\partial R_{xx}/\partial V_{\mathrm{G}} \propto \partial V_x/\partial V_{\mathrm{G}}$, is studied by applying a dc current of 500 pA and modulating the gate-bias voltage with the peak-to-peak amplitude of 250 μV.

III. EXPERIMENTAL RESULTS

Figure 1 shows the four-terminal longitudinal resistance $R(V_{\mathrm{GL}},V_{\mathrm{GR}})$ as a function of gate-bias voltage V_{G} taken on a sample ($L=W=3$ μm, wafer I). We apply V_{G} to only one of the gates (V_{GL} or V_{GR}) at a fixed magnetic field of $B=2.5$ T, corresponding to the Landau-level filling factor of $\nu=4$. In this condition, the 2DEG region outside the gates act as perfect leads. The 2DEG region underneath the biased gate, which serves as a scattering region, undergoes a transition from the $\nu=4$ to the $\nu=3$ IQH states and exhibits distinct fluctuations. The RF's are reproducible and specific to the regions studied. This is true for all the samples studied. We mention that the distinct RF was not visible when L (W) exceeds 10 μm.

The inset of Fig. 1 shows temperature dependence of the IQH transition. The amplitude of RF's diminishes with increasing temperature T, and RF's become invisible at $T>640$ mK. We have confirmed in additional studies that the inelastic-scattering length L_{in} largely exceeds the size of the conductor (L, W).[16] We are, hence, confident that the coherence is maintained in individual scattering regions.

To explicitly test if the RF's are a consequence of coherent interference of electron waves, we connect the two scattering regions through the 2DEG in an IQH state. This can be done by biasing the two gates (V_{GL} and V_{GR}) simultaneously. Our previous studies have demonstrated that the inelastic-scattering length of edge states in IQH states well exceeds 1 mm.[17,18] In the present configuration ($L_{\mathrm{edge}}=10$ μm), therefore, it is certain that the electron waves propagate back and forth between the two scattering regions, maintaining their phase memory. Thus, the RF's are expected to change to yield a pattern that cannot be simply related to the original patterns of respective individual regions if the RF's originate from coherent processes.

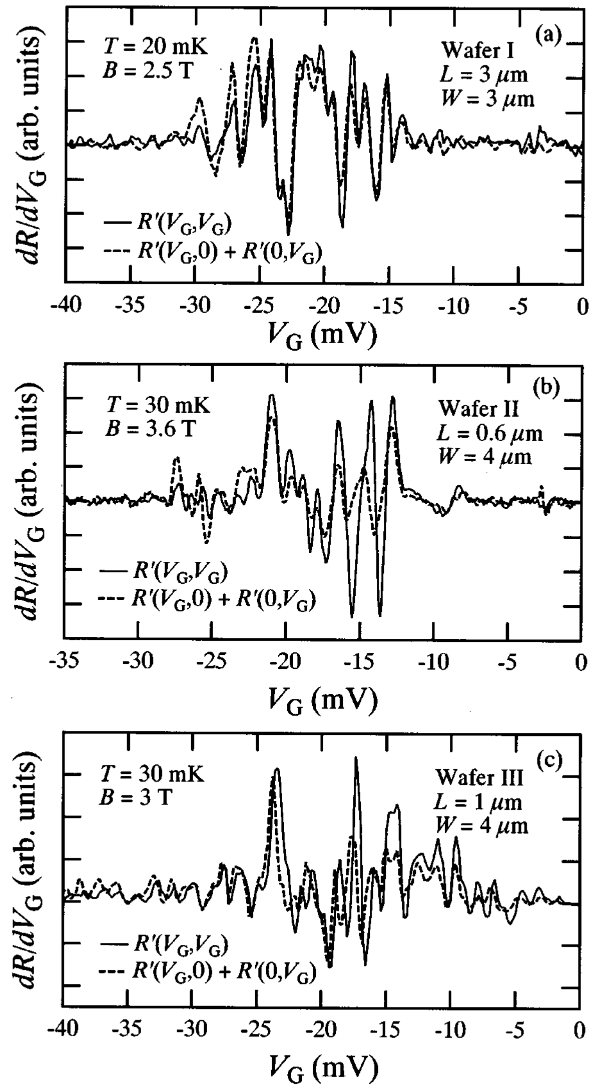

FIG. 2. IQH transition for the total system in differential resistance $R'(V_{\mathrm{G}},V_{\mathrm{G}})$, obtained by biasing both of the gates GL and GR simultaneously (solid line). The numerical sum of the single-gate spectrum for GL and that for GR (dashed line). (a) $L=W=3$ μm, wafer I. (b) $L=0.6$ μm, $W=4$ μm, wafer II. (c) $L=1$ μm, $W=4$ μm, wafer III.

Figure 2(a) displays fluctuation patterns on the sample used in Fig. 1 ($L=W=3$ μm, wafer I) in the differential longitudinal resistance $\partial R_{xx}/\partial V_{\mathrm{G}} \equiv R'(V_{\mathrm{GL}},V_{\mathrm{GR}})$. The transition is from the $\nu=4$ IQH state to the $\nu=3$ IQH state as in Fig. 1. When either one of the gates (V_{GL} or V_{GR}) is biased, $R'(V_{\mathrm{G}},0)$ or $R'(0,V_{\mathrm{G}})$ exhibits distinct RF's as has been shown in Fig. 1. The dashed line in Fig. 2(a) shows the numerical sum of the two, $R'(V_{\mathrm{G}},0)+R'(0,V_{\mathrm{G}})$. The solid line in Fig. 2(a) shows $R'(V_{\mathrm{G}},V_{\mathrm{G}})$, obtained by biasing GL and GR simultaneously. Note that the intermediate 2DEG region between the two regions is fixed in the $\nu=4$ IQH

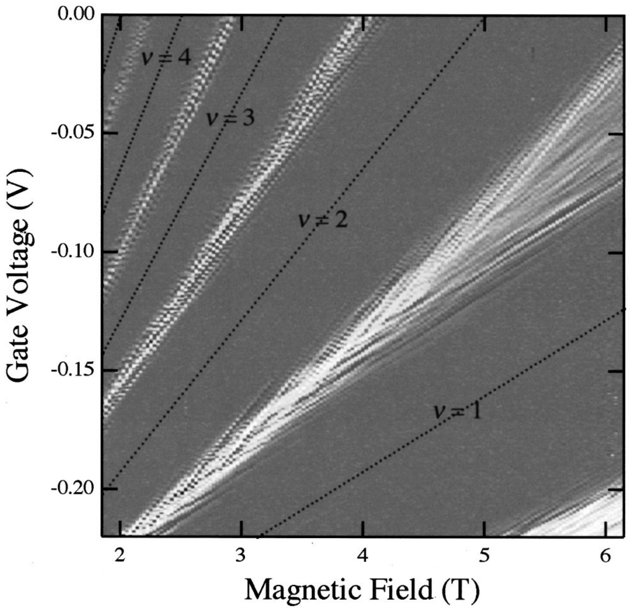

FIG. 3. Gray-scale plot of differential resistance in sweep of V_G and B. Lighter color represents larger value. The dark dotted lines represent integer filling of Landau level.

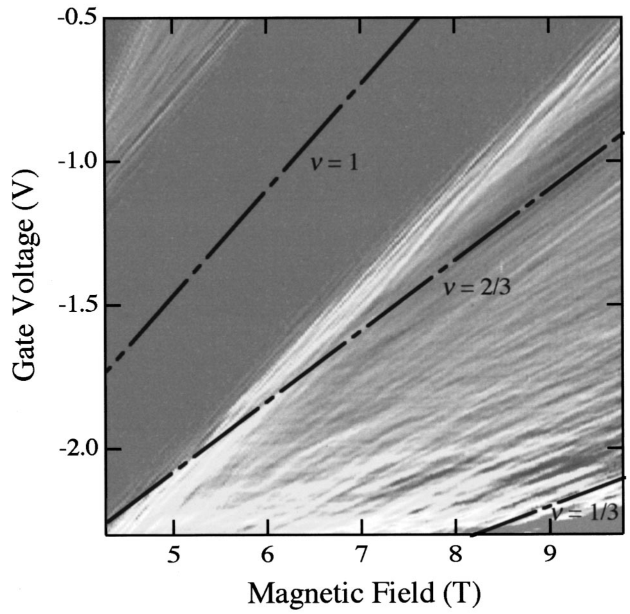

FIG. 4. Gray-scale plot of differential resistance in sweep of V_G and B. Lighter color represents larger value. The dark dashed-and-dotted lines represent integer and fractional filling of Landau level.

state to assure coherent interaction between electron waves in the two scattering regions. The RF's shown in Fig. 2(a) have the following two unexpected but distinct features. (A) The RF pattern of the connected system (solid line) closely resembles the one obtained by classically adding the resistance of each region (dashed line). However, (B) they are not exactly the same; the amplitude of the RF's in the total system (solid line) is distinctly enhanced on the higher-energy side in the transition region ($V_G > -23$ mV), while it is suppressed on the lower-energy side ($V_G < -23$ mV).

These two features have been found to be true in all the samples and also for different IQH transitions. Two additional examples are displayed in Figs. 2(b) and 2(c), where the $\nu = 4 \leftrightarrow 3$ transition on another sample ($L = 0.6$ μm, $W = 4$ μm, wafer II) and on yet another sample ($L = 1$ μm, $W = 4$ μm, wafer III) are shown, respectively.

We note that feature (B) in the above is consistent with our earlier findings,[17] and shows that the two scattering regions interact quantum-mechanically. Thus we are led to the conclusion that the RF patterns are substantially determined by a classical origin (A) whereas the electron system is in a coherent regime (B).

To gain a hint of the physical picture of RF's, we show in Fig. 3 a gray-scale plot of the differential resistance by biasing one gate (V_{GL}) on a sample ($L = W = 3$ μm, wafer I) as a joint function of B and V_G. Peaks and dips in the RF's are indicated by the dark and bright regions, respectively. The black dotted lines mark the values of B and V_G, which correspond to integer filling factors ($\nu = 1$, 2, 3, and 4). The trajectories of the RF extrema in every transition region ($n - 1 < \nu < n$) are classified into two groups of parallel tracks, one having the slope of $\nu = n$ and the other of $\nu = n - 1$. The former is dominant when the Fermi level is above the center of Landau level and the latter is dominant below the level center, while both groups of trajectories coexist in neighborhood of level center. These features are similar to the trajectories reported for the conductance fluctuations in IQH transitions on Si-MOSFET devices.[15]

Figure 4 shows a similar gray-scale plot in a range of higher magnetic fields, where the black dash-and-dotted lines mark the integer and the fractional filling factors ($\nu = 1$, 2/3, and 1/3). RF's are observed in the transition regions, $\nu = 1 \leftrightarrow 2/3$ and $\nu = 2/3 \leftrightarrow 1/3$. The trajectories in the region $\nu = 1 \leftrightarrow 2/3$ clearly follow straight lines parallel to either $\nu = 1$ or $\nu = 2/3$. In the transition region, $\nu = 2/3 \leftrightarrow 1/3$, similar trends are also noted. It is hence suggested that the RF's in FQH transitions may have an analogous physical origin.

IV. DISCUSSION AND INTERPRETATION

We begin by noting fundamental aspects of the present experimental observations. First, the thermal length $L_T = (hD/k_B T)^{\frac{1}{2}}$ (Refs. 1 and 2) is estimated to be 0.66 μm in the present experimental condition ($T = 30$ mK). Since $L_T < L$ for most of the samples studied, UCF-like fluctuations may tend to smear. Second, the characteristic period of the presently observed RF's in the sweep of V_G [Figs. 1 and 2(a)–2(c)] is roughly about $\delta V_G \approx 2$ mV, which corresponds to a Fermi-energy change of $\delta\epsilon_F \approx 50$ μeV in the 2DEG system. This energy interval is roughly 50–120 times larger than the typical level separation defined as the inverse of the density of states for respective scattering regions; in other words, 50–120 electrons are added to or extracted from the scattering region underneath the gate for each fluctuation period. This observation is consistent with the smearing out of the RF's at $T > 640$ mK (the inset of Fig. 1), where the thermal energy $k_B T$ exceeds this energy interval $\delta\epsilon_F$. Hence, the presently observed RF's are an effect that survives after av-

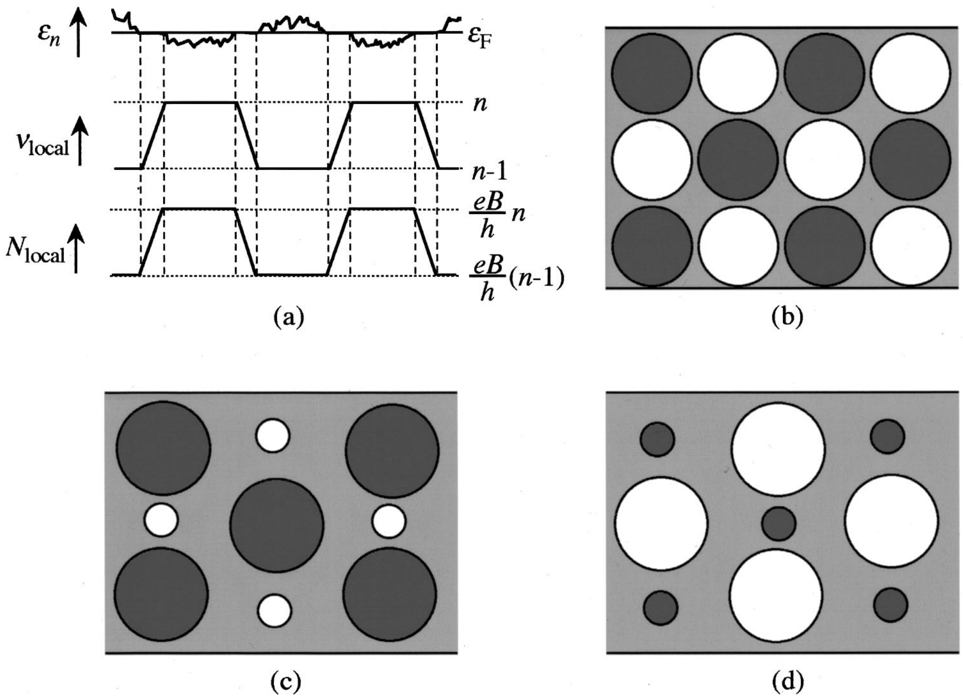

FIG. 5. (a) Schematic representation of the Landau-level energy, the local filling factor, and the local electron density. (b)–(d) Schematic representation of electron systems in high magnetic fields. It breaks up into incompressible regions in $\nu=n$ IQH state (dark shaded) and incompressible regions in $\nu=n-1$ IQH state (white), which are surrounded by compressible regions (light shaded). (b) Near the level center of Landau level. (c) Above the level center. (d) Below the level center.

eraging 50–120 electron levels and not a signature of a single level. Finally, we expect nevertheless that one-electron level is well defined in each scattering region. Each level may be affected when it is brought into quantum-mechanical interaction with other levels by the connection of two scattering regions with dissipationless edge states. This must occur in the present experiments. However, the possible modification in energy may be level specific and its signature and amplitude may be randomly distributed with a typical size on the order of the average level separation. Hence, such an effect of eigenstate modification due to interaction is not expected to give rise to a directly visible signature in the experiments. This view is consistent with the conclusion derived from features (A) and (B) in the above that the RF patterns are of a classical origin although the electron system is coherent.

We now consider possible interpretation of the RF's. Detailed electronic structures of 2DEG system in IQH regimes have been directly visualized by recent imaging techniques.[19,20] The observations, however, have been limited to IQH plateau regions, where ν is close to integer values and the global diagonal conductance of the electron system is vanishing. In IQH transition regions with ν well away from an integer, as in the present experiments, only featureless and uniform images are obtained in the local probing technique.[19] We note that this does not imply the absence of electronic structure in IQH-transition regions but simply indicates the consequence of a nonvanishing conductance (or the screening capability) of the 2DEG systems. As described below, we expect characteristic structures also in QH-transition regions.

Let us consider a finite coherent 2DEG system in an IQH-transition region ($\nu=n\leftrightarrow n-1$), where the global diagonal conductance is finite. If random potentials are ignored, the topmost nth Landau level (LL) energy, ϵ_n, must be completely uniform in space (except in the vicinity of edges), nesting exactly at the Fermi level, ϵ_F. Random potentials may be strongly suppressed when compared to those in IQH-plateau regions because of effective screening effects. However, they can never be ignored in true 2DEG systems. In the presence of slowly varying small potential fluctuations, ϵ_n will fluctuate in space around ϵ_F, approximately reproducing the landscape of the potential fluctuation. We expect that the fluctuation amplitude is smaller than the LL splitting as well as the spin-splitting energy. At low temperatures, the nth LL will then be completely filled in the fractional regions where $\epsilon_n<\epsilon_F$, while it is empty in the other fractional regions where $\epsilon_n>\epsilon_F$. Such regional distinction may be done with a resolution of the magnetic length l_B, which is typically 0.01 μm and much smaller than the size of the 2DEG system considered here. Accordingly, the 2DEG system splits into the two classes of incompressible subregions with the local filling factors quantized to $\nu_{local}=n$ and $\nu_{local}=n-1$ [with the local electron densities $N_{local}=(eB/h)\nu_{local}$ (h is the Planck constant)] as shown in Fig. 5(a). These incompressible subregions are nonconducting and are separated to one another by compressible regions in which $\epsilon_n=\epsilon_F$ ($n-1<\nu_{local}<n$). The compressible regions form a conductive network,[21] tracing the regions where the scattering-wave states[22,23] have finite probability amplitudes in the disordered coherent 2DEG system. Accordingly, the network must traverse the entire region of the finite electron system because the global (diagonal) conductance is assumed to be finite.[24] It follows that each incompressible subregion must form either an isolated *lake* ($\nu_{local}=n$) or an isolated *island* ($\nu_{local}=n-1$) completely surrounded by compressible regions, as schematically illustrated in Fig. 5(b).[25]

At the middle of the transition region, $\nu=n-1/2$, the Fermi level ϵ_F will define the center of the locally fluctuating

ϵ_n [Fig. 5(a)], so that the *lakes* ($\nu_{\rm local}=n$) and the *islands* ($\nu_{\rm local}=n-1$) may have nearly equal weights as shown in Fig. 5(b).[26] In the upper half region of the transition, $\nu>n-1/2$, where $\epsilon_{\rm F}$ is above the level center, the *lakes* ($\nu_{\rm local}=n$) will dominate the *islands* ($\nu_{\rm local}=n-1$) as shown in Fig. 5(c). The opposite feature is expected in the lower-half region of the transition, $\nu<n-1/2$ as shown in Fig. 5(d). We suppose that the topological network pattern of the compressible regions substantially determines the conductance value. Particularly, in the upper-half region of the transition, the conductance will be most sensitively affected by the topological feature of the *lakes*. Similarly, in the lower half region of the transition, that of the *islands* will be important.

Our interpretation of the RF's is as follows. When $V_{\rm G}$ increases, electrons have to be added to the electron system. The added electrons modify the potential profile through screening effect. We suppose that the potential-fluctuation pattern or the shape of the compressible-strip network is sensitively affected by a small change in $V_{\rm G}$. Therefore, varying $V_{\rm G}$ causes the shape of the *lakes* and the *islands* to change irregularly, that in turn affects the conductance. This is the origin of the RF's. This picture is supported by the direct observation of the potential topography in IQH-plateau regions, which demonstrates a profound change in the potential profile upon a small perturbation:[20] In the QH-transition regions, the pattern change may be equally profound even though the amplitude change of local potentials may be much smaller.

Now we explain why the extrema of the RF's in the $V_{\rm G}$-B plane trace straight lines parallel to the lines of $\nu=n$ and $\nu=n-1$. When we increase both $V_{\rm G}$ and B starting from certain values so as to trace a trajectory parallel to the line of $\nu = n$, the ratio of the increments in $V_{\rm G}$ and B satisfies $\Delta V_{\rm G}/\Delta B=ne^2/hC$, where C is the capacitance per unit area between the gate and the 2DEG. The local electron density $N_{\rm local}$ at a location (x,y) increases by $\Delta N=C\Delta V_{\rm G}/e$ when $V_{\rm G}$ increases by $\Delta V_{\rm G}$. Noting the relation $\nu_{\rm local}=N_{\rm local}/(eB/h)$, we can find that $\nu_{\rm local}$ does not change during this process if $\nu_{\rm local}$ is originally equal to n, but increases if $\nu_{\rm local}$ is originally smaller than n. It immediately follows that each incompressible *lake* ($\nu_{\rm local}=n$) is kept unchanged both in shape and size whereas each incompressible *island* ($\nu_{\rm local}=n-1$) shrinks in size.[27] We suggest that this explains why the RF extrema mainly trace straight lines parallel to $\nu=n$.

If $V_{\rm G}$ and B increase so as to trace a line parallel to $\nu=n-1$, we can conclude through similar consideration that each *lake* ($\nu_{\rm local}=n$) shrinks in size while the topological feature of each *island* ($\nu_{\rm local}=n-1$) is kept unchanged. This explains why the RF extrema in the lower half region of the transition mainly trace straight lines parallel to $\nu=n-1$. In an intermediate region around $\nu=n-1/2$, the topology determined by both of the *lakes* and the *islands* is important and the trajectories of the RF extrema parallel to $\nu=n$ and $\nu=n-1$ coexist.

Our simplified model in the above thus explains all the observed features by assuming that the 2DEG system splits into isolated incompressible *lakes* ($\nu_{\rm local}=n$) and isolated incompressible *islands* ($\nu_{\rm local}=n-1$), which are separated by compressible regions ($n-1<\nu_{\rm local}<n$). From similar experimental features of FQH transitions of $\nu=1\leftrightarrow2/3$ and $\nu=2/3\leftrightarrow1/3$ (Fig. 4), we conjecture that the 2DEG system in FQH-transition regions splits into isolated incompressible *lakes* ($\nu_{\rm local}=p$) and isolated incompressible *islands* ($\nu_{\rm local}=p'$), which are separated by compressible regions ($p'<\nu_{\rm local}<p$), where $(p,p')=(1,2/3)$ or (2/3, 1/3).

We finally comment on the work of Cobden and co-workers,[15] which suggests that the fluctuations arise from the charging effect.[28] As described above, our interpretation is different. Aside from the difference in the models assumed,[25] we mention the following. First, even if Coulomb blockade takes place in one particular site (either in an isolated incompressible *lake* or *island*), it appears to be difficult that the blockade substantially influences the global conductance of the 2DEG system because the conduction may be readily bypassed in the network of percolating compressible regions. If, nevertheless, one particular site is assumed to occasionally give a bottleneck of conduction, the conductance would oscillate with a much shorter period than those found in the experiments because the sequential addition (extraction) of electrons to (from) the particular site should then be visible. Second, the charging model accounts for the existence of the trajectories parallel to $\nu=n$ but does not explain the existence of those parallel to $\nu=n-1$. Finally, the featureless images obtained in the local probing technique[19] may suggest that the Coulomb-blockade-like behavior is difficult to occur in the QH-transition regions.

V. SUMMARY

We have studied RF's in IQH transitions to examine the role of coherence. The experiments indicate that the coherence does not play a substantial role in determining the pattern of the RF's even though the electron system is coherent. We suggest that a 2DEG system in IQH transition splits into isolated incompressible *lakes* ($\nu_{\rm local}=n$) and isolated incompressible *islands* ($\nu_{\rm local}=n-1$), which are separated by compressible regions ($n-1<\nu_{\rm local}<n$), and that an irregular change in the topology of these regions gives rise to the RF's. A similar break up of the 2DEG system into different subregions is also suggested for FQH transitions.

[1] Y. Imry, *Introduction to Mesoscopic Physics* (Oxford University press, New York, 1997).
[2] P.A. Lee and A.D. Stone, Phys. Rev. Lett. **55**, 1622 (1985).
[3] B. Jovanović and Z. Wang, Phys. Rev. Lett. **77**, 4426 (1996).
[4] S. Cho and M.P.A. Fisher, Phys. Rev. B **55**, 1637 (1997).
[5] S. Xiong and A.D. Stone, Phys. Rev. Lett. **68**, 3757 (1992).
[6] D.L. Maslov and D. Loss, Phys. Rev. Lett. **71**, 4222 (1993).
[7] A.G. Galstyan and M.E. Raikh, Phys. Rev. B **56**, 1422 (1997).
[8] T. Ando, Phys. Rev. B **49**, 4679 (1994).
[9] H.-Y. Kee, Y.B. Kim, E. Abrahams, and R.N. Bhatt, Phys. Rev. B

58, 12 605 (1998).
[10] A. Morgan, D.H. Cobden, M. Pepper, G. Jin, Y.S. Tang, and C.D.W. Wilkinson, Phys. Rev. B **50**, 12 187 (1994).
[11] J.A. Simmons, H.P. Wei, L.W. Engel, D.C. Tsui, and M. Syayegan, Phys. Rev. Lett. **63**, 1731 (1989).
[12] P.C. Main, A.K. Geim, H.A. Carmona, C.V. Brown, T.J. Foster, R. Taboryski, and P.E. Lindelof, Phys. Rev. B **50**, 4450 (1994).
[13] J.K. Jain and S.A. Kivelson, Phys. Rev. Lett. **60**, 1542 (1988).
[14] M. Büttiker, Phys. Rev. B **38**, 12 724 (1988).
[15] D.H. Cobden, C.H.W. Barnes, and C.J.B. Ford, Phys. Rev. Lett. **82**, 4695 (1999); D.H. Cobden and E. Kogan, Phys. Rev. B **54**, 17 316 (1996).
[16] T. Machida, H. Hirai, S. Komiyama, and Y. Shiraki, Phys. Rev. B **54**, 16 860 (1996).
[17] T. Machida, H. Hirai, S. Komiyama, T. Osada, and Y. Shiraki, Solid State Commun. **103**, 441 (1997).
[18] T. Machida, H. Hirai, S. Komiyama, and Y. Shiraki, Physica B **249-251**, 128 (1998).
[19] S.H. Tessmer, P.I. Glicofridis, R.C. Ashoori, L.S. Levitov, and M.R. Melloch, Nature (London) **392**, 51 (1998).
[20] G. Finkelstein, P.I. Glicofridis, R.C. Ashoori, and M. Shayegan, Phys. Rev. B **61**, 16 323 (2000).
[21] D.B. Chklovskii and P.A. Lee, Phys. Rev. B **48**, 18 060 (1993).
[22] M. Büttiker, IBM J. Res. Dev. **32**, 317 (1988).
[23] S. Komiyama and H. Hirai, Phys. Rev. B **54**, 2067 (1996).
[24] In an infinitely large system, the compressible strips cannot percolate over a region larger than the localization length, which is predicted to be finite except at exactly $\nu = n - 1/2$. However, we consider a finite system in the transition region, where the localization length exceeds the system size. This is why the compressible strips traverse the entire region here.
[25] Our model is different from the charging picture suggested by Cobden and co-workers (Ref. 15), in which the profile of an electron density fluctuation is assumed to be substantially unaffected by B. Furthermore, it is argued that isolated metallic (compressible) puddles are completely surrounded by insulating (incompressible) strips, which is opposite to the view of our model.
[26] In a real 2DEG system, the shape of incompressible regions will have more complicated shape. However, the simplification in our picture does not affect the argument in this study.
[27] For each *island*, the total number of holes in the nth LL is kept unchanged despite the size shrinkage.
[28] L. P. Kouwenhoven, C. M. Marcus, P. L. McEuen, S. Tarucha, R. M. Westervelt, and N. S. Wingreen, in *Mesoscopic Electron Transport*, edited by L. L. Sohn, L. P. Kouwenhoven, and G. Schön (Kluwer Academic, Dordrecht, Netherlands, 1997), p. 105.